Applied Energy xxx (xxxx) xxx–xxx

Contents lists available at ScienceDirect

Applied Energy

journal homepage: www.elsevier.com/locate/apenergy

Optimal supply and demand bidding strategy for an aggregator of small prosumers

José Iria[a,b,*], Filipe Soares[a], Manuel Matos[a,b]

[a] Centre for Power and Energy Systems (CPES), INESC TEC, Porto, Portugal
[b] Faculty of Engineering of University of Porto (FEUP), Porto, Portugal

HIGHLIGHTS

- Participation of an aggregator of small prosumers in the energy market.
- The aggregator exploits the flexibility of prosumers' appliances, in order to reduce market net costs.
- A two-stage stochastic optimization model to define demand and supply bids for the day-ahead energy market is presented.
- A model predictive control method to set the operation of flexible loads in real-time is presented.
- A case study of 1000 small prosumers from the Iberian market is used to compare the proposed methods to other benchmarks.

ARTICLE INFO

Keywords:
Aggregator
Electricity markets
Model predictive control
Prosumers
Two-stage stochastic optimization

ABSTRACT

This paper addresses the problem faced by an aggregator of small prosumers, when participating in the energy market. The aggregator exploits the flexibility of prosumers' appliances, in order to reduce its market net costs. Two optimization procedures are proposed. A two-stage stochastic optimization model to support the aggregator in the definition of demand and supply bids. The aim is to minimize the net cost of the aggregator buying and selling energy at day-ahead and real-time market stages. Scenario-based stochastic programing is used to deal with the uncertainty of electricity demand, end-users' behavior, outdoor temperature and renewable generation. The second optimization is a model predictive control method to set the operation of flexible loads in real-time. A case study of 1000 small prosumers from the Iberian market is used to compare four day-ahead bidding strategies and two real-time control strategies, as well as the performance of combined day-ahead and real-time strategies. The numerical results show that the proposed strategies allow the aggregator to reduce the net cost by 14% compared to a benchmark typically used by retailers (inflexible strategy).

1. Introduction

1.1. Motivation

Demand response is acknowledged as the inevitable solution to enhance the economic effectiveness of electricity markets, increase the integration of renewable energy resources and improve the operation of electric power systems [1]. Several countries have already established demand response programs that harness the largest and most energy intensive industrial and commercial clients through dynamic tariff schemes or direct use of load, as part of their system balancing activities [2]. According to the international energy agency, industrial users consume 32.1% of the total electricity demand in the developed countries, whereas commercial services and residential consumers account for 31.8% and 32.2%, respectively. Large consumers are already considered as a flexibility resource, while the major share of electricity consumption, small services and residential consumers, remain untapped. However, the recent advances in real deployment of smart home and grid technologies promise to leverage once and for all the active participation of small consumers in demand response programs [3,4]. The smart home technologies include automation solutions, such as home energy management systems (HEMS), photovoltaic (PV) systems and smart appliances with communication, monitoring and control functionalities. Therefore, the technical barriers of demand response are no longer on the side of the automation solutions. The main challenge is to transform these automation functionalities into products that can be traded by an aggregator in the electricity markets.

* Corresponding author at: Centre for Power and Energy Systems (CPES), INESC TEC, Porto, Portugal.
E-mail address: jpiria@inesctec.pt (J. Iria).

http://dx.doi.org/10.1016/j.apenergy.2017.09.002
Received 14 June 2017; Received in revised form 11 August 2017; Accepted 2 September 2017

Nomenclature

Abbreviations and Superscripts

AR/DE	arrival/departure of electric vehicles
DA	day-ahead
EV	electric vehicle
$HEMS$	home energy management system
INL	inflexible net load
MPC	model predictive control
PV	photovoltaic
RT	real-time
SL	shiftable load
TCL	thermostatically controlled load
$\hat{}$	point forecast
$\underline{\vee}$,$\overline{\wedge}$	load, generation
$+$,$-$	positive, negative imbalances

Indices and Sets

$j \in S$	scenarios
$t,k,w \in H$	time interval
$v \in \{EV, TCL, SL, INL\}$	type of load
$i \in L^v$	loads
$H^v \subset H$	sub-set of time intervals
$O \subset H$	set of time intervals of active occupancy
	availability to start $\underline{H}^{SL}$ and complete $\overline{H}^{SL}$ a working cycle (sets)
$y \in N$	prosumers

Parameters

C	thermal capacitance (kWh/°C)
COP	coefficient of performance
CP	contracted power (kW)
D	number of time intervals of a working cycle
$\overline{E}$	maximum energy (kWh)
$\overline{P}$	maximum electric power (kW)
Pr	power profile (kW)
$\overline{SOC}$,$\underline{SOC}$	maximum, minimum state-of-charge (kWh)
R	thermal resistance (°C/kW)
λ	price (€/kWh)
π	probability of occurrence of the scenarios
η	efficiency
$\Delta t,\Delta k$	duration of time interval $t(1h),k(0.25h)$
$\overline{\theta}$, $\underline{\theta}$	maximum, minimum temperature (°C)
θ^o	outdoor temperature (°C)

Variables

E	energy (kWh)
I	imbalance (kWh)
P	electric power (kW)
SOC	state-of-charge (kWh)
θ	temperature (°C)
ψ	sets the beginning of a working cycle (binary)
$\varnothing$	auxiliary (binary)

1.2. Related work

The participation of aggregators in the day-ahead (DA) energy market has been the focus of many recent studies. In the electric mobility context, Bessa et al. [5,6] proposed two deterministic optimization models to define demand bids, based on point forecasted information of electric vehicles (EV) mobility patterns and energy prices. Kristoffersen et al. [7] included battery wear costs in the DA optimization of EV charging. Vagropoulos and Bakirtzis [8] proposed a two-stage stochastic model to optimize demand bids, considering the uncertainty of EV mobility patterns and electricity prices through scenarios. Mohsenian-Rad [9] extended the aggregator portfolio to other shiftable loads (SL), such as dishwashers and washing machines. A time-coupled stochastic optimization problem was formulated to select price and demand bids to the DA market and demand bids to the real-time (RT) market. Ayón et al. [10] presented a deterministic model to optimize demand bids for the DA energy market, based on forecasted load flexibility. Under the assumption of direct control over thermostatically controlled loads (TCL), Chen et al. [11] proposed a stochastic model to define DA demand bids, based on scenarios of DA energy prices. Babar et al. [12] formulated an applied methodology for an agile demand response using micromodels. The objective is to optimize demand flexibility to be traded by an aggregator in the DA market. Saez-Gallego et al. [13] developed a billevel optimization model that uses price-consumption data to define demand bids that capture the price-response of consumers.

Another group of papers has presented strategies to control aggregated flexible resources, in order to comply with DA market commitments. Many of these studies are focused on TCL [14–17]. For example, Perfumo et al. [14] developed a model-based feedback control strategy for load management of large groups of TCL. Mathieu et al. [15] explored state estimation and control methods to manage RT energy imbalances. The authors also investigated how various levels of monitoring and communications infrastructure affect the aggregated control of TCL. Callaway [16] developed new methods to model and control aggregated TCL with the objective of delivering regulation services. Zhou et al. [17] proposed a two-level scheduling method to reduce imbalance costs through the control of aggregated TCL. This approach considers a model predictive control (MPC) optimization in the upper level to set the aggregated demand and a priority list strategy in the lower level to define ON/OFF set-points. Subramanian et al. [18] developed scheduling algorithms to coordinate populations of SL and storage devices, in order to minimize reserve deployment costs. Bessa et al. [5] proposed a management procedure based on deterministic optimization to set the operation of an EV fleet. In the topic of virtual power plants, Vasirani et al. [19] presented a MPC approach that uses the flexibility of EV to compensate the intermittent generation of wind farms.

1.3. Contributions

The expected transformation of consumers into prosumers in the coming years creates an opportunity for an aggregator to exploit distributed energy resources (i.e., loads and generators) as single products in the electricity market. This paper presents a framework to enable the participation of an aggregator of small prosumers on both sides of the energy market. The aggregator relies on the agility of the smart home appliances to provide flexibility and respond to fast market variations without compromising the energy needs and preferences of the prosumers. This load agility concept was proposed by Babar et al. in [12,20] and is known as agile demand response.

The contributions of this paper are two optimization models. The first contribution corresponds to a two-stage stochastic optimization model to support the aggregator in the definition of demand and supply bids to submit to the DA energy market. The aim is to minimize the net cost of the aggregator buying and selling energy in the DA and RT market stages. The bids result from the optimization of flexible and inflexible net load (INL). The flexible net load includes EV, TCL and SL.

The INL includes renewable generation and inflexible load. Scenario-based stochastic programing is used to tackle the uncertainties of end-users' behavior, renewable generation, electricity load and outdoor temperature. The proposed approach differs from others [5–13] by considering the participation of the aggregator in the supply and demand side of the DA energy market and by including different sources of flexibility and uncertainty in the joint optimization of demand and supply bids.

The second contribution fulfils one of the gaps of [6–12] by considering a RT management phase, where the aggregator sets the operation of the flexible loads. A MPC method based on deterministic optimization is proposed to dispatch the flexible loads in a way that minimizes the net cost of buying and selling energy in RT. This approach differs from the above mentioned methods [5,14–19] in various ways. First, it considers the control of different types of flexible resources (EV, SL and TCL), which makes its mathematical formulation very different. Compared with the direct load control methods presented in [14–16,18], the proposed approach assists an aggregator to arbitrage and thus contributes to balance the system in an indirect way. Moreover, it exploits the aggregated load flexibility of the prosumers to mitigate demand and generation imbalances, contrarily to other works that are only focused on demand [5] or generation [19] imbalances.

In short, the proposed approaches allow prosumers to value their load flexibility and generation surplus by transforming them into market products. The adoption of these strategies may avoid prosumers from investing in dedicated storage devices to store excess of renewable generation.

The proposed bidding strategy is compared to other three benchmarks characterized by different bid optimization procedures (deterministic [5–7,10] and inflexible models) and different forms of dealing with uncertainty (point and perfect forecasted data). The RT control strategy is compared to one benchmark, whose objective is to minimize energy imbalances. Furthermore, the combined performance of DA and RT strategies is also evaluated. A case study of 1000 small prosumers from the Iberian market (MIBEL) is used to perform these analyzes.

1.4. Paper organization

The remaining paper is organized as follows. Section 2 describes the aggregator framework. Section 3 presents the DA optimization model. Section 3 describes MPC method. The case study and results are presented in And 56. Finally, Section 7 presents the conclusions.

2. Participation of the aggregator in the energy market

2.1. Energy market framework

The participation of the aggregator in the DA energy market follows the rules of the MIBEL [21]. However, the methodologies described in this paper can be applied to other markets without substantial changes (e.g., EPEX, ELSPOT from Nord Pool or PJM).

The MIBEL covers the Portuguese and Spanish control areas. The DA energy market has a uniform price and double-side auction. The market agents may present buy and sell hourly bids that cover all 24 h of the next day. The bid prices can go from 0 up to 180 €/MWh, and the bid quantities must be greater than 0.1 MWh. The volume of energy and price of each hour are defined by the point of intersection between the supply and demand curves, according to the EUPHEMIA algorithm [22]. The gate closure occurs at 12th hour and the clearing prices are published at 13th hour. Before the 14th hour, the physical bilateral contracts are added to the cleared offers. Between the 14th and 16th hours, the transmission system operator performs congestion management analysis, and then proceeds to the generation of viable daily schedules. In case of being detected any network problem, market mechanisms are activated (e.g., market splitting). Fig. 1 shows the timeline of these two market sessions.

The energy deviations between RT realizations and DA market commitments are valued at imbalance prices. The methodologies to define imbalance prices are diverse and depend mainly on the regulation mechanisms of each country and market. The imbalance prices in Portugal and Spain result from complex functions of energy and regulation prices, as described in [23,24]. In other markets, such as Nord Pool and PJM, the two-price settlement mechanism is adopted. This mechanism values energy deviations that support the system at energy prices, and deviations that put the system off-balance at manual reserve prices in case of the Nord Pool [25], and at RT prices in case of the PJM market [8,26].

The cost and revenue of buying and selling energy are computed by Eqs. (1) and (2). The first term of Eqs. (1) and (2) defines the cost and revenue of buying $E_t^{DA,\vee}$(kWh) and selling $E_t^{DA,\wedge-}$ energy at energy price λ_t^E(€/kWh) in the DA market. The second term defines the imbalance cost, due to deviations between DA market commitments and RT realizations of load $E_t^{RT,\vee}$ and generation $E_t^{RT,\wedge-}$. The imbalances I_t (kWh) are valued at positive λ_t^+(€/kWh) and negative λ_t^- imbalance prices. Typically, $\lambda_t^- \geqslant \lambda_t^E$ and $\lambda_t^+ \leqslant \lambda_t^E$.

$$Cost = \sum_t \lambda_t^E E_t^{DA,\vee} + \begin{cases} \lambda_t^+ I_t^{\vee}, I_t^{\vee} < 0 \\ \lambda_t^- I_t^{\vee}, I_t^{\vee} \geqslant 0 \end{cases} \quad (1)$$

$$Revenue = \sum_t \lambda_t^E E_t^{DA,\overline{\wedge}} + \begin{cases} \lambda_t^- I_t^{\wedge-}, I_t^{\wedge-} < 0 \\ \lambda_t^+ I_t^{\wedge-}, I_t^{\wedge-} \geqslant 0 \end{cases} \quad (2)$$

$$I_t^{\vee} = E_t^{RT,\vee} - E_t^{DA,\vee} \quad (3)$$

$$I_t^{\overline{\wedge}} = E_t^{RT,\overline{\wedge}} - E_t^{DA,\overline{\wedge}} \quad (4)$$

2.2. Aggregator framework

The aggregator assumes the role of retailer and supplier, since it buys and sells energy. It exploits the flexibility of the prosumers' resources to decrease its costs in the energy market. In exchange, the aggregator may offer attractive tariffs or monthly discounts in the electricity bill (e.g., [11]). The remuneration mechanisms of the aggregator are out of the scope of this paper and will be addressed in future work.

The aggregator acts as a price taker by submitting non-priced demand and supply bids to the DA energy market. This means that demand bids are submitted at market cap price (180 €/MWh), whereas supply are presented at floor price (0 €/MWh). Fig. 1 shows a diagram with the sequence of aggregator's tasks. Before the 12th hour, the aggregator defines and submits the demand and supply bids. During the operating day, the aggregator sets the operation of the flexible loads. The optimization procedures to define the energy bids and to control the operation of the flexible loads in RT are described in Sections 3 and 4, respectively.

Fig. 2 describes the hierarchical management and control structure adopted in this paper. Similar frameworks were proposed by the European projects VIMSEN [27] and SEMIAH [28].

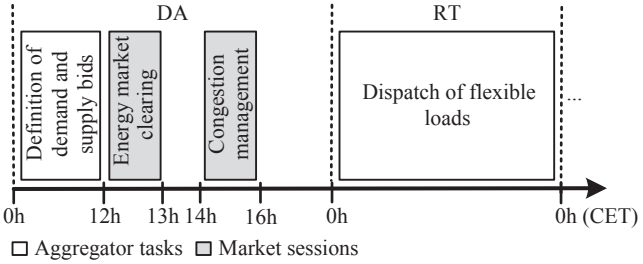

Fig. 1. Diagram with the sequence of aggregator's tasks and relevant market sessions, based on MIBEL timeline [21].

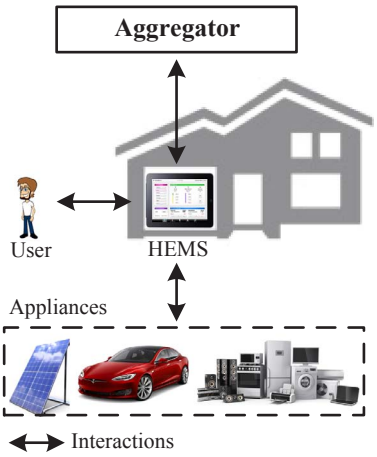

Fig. 2. Hierarchical management and control structure.

The aggregator interfaces with the prosumers through a HEMS installed by it. The HEMS is responsible for acquiring and processing data collected from appliances (e.g., sensors and smart loads), monitoring and controlling flexible appliances, as well as establishing interactions between the aggregator, users and appliances. The users interact with the HEMS through a smartphone application. More details about the HEMS functionalities required in the DA and RT stages are provided in Sections 3.1 and 4.1.

3. Day-ahead bidding optimization

3.1. System architecture and information chain

For the short-term time horizon (up to 48 h ahead), the aggregator buys and sells energy in DA market. The aggregator exploits the flexibility of the AC, TCL and SL, based on information collected from the HEMS of each prosumer. Fig. 3 describes the system architecture and information chain. At the beginning of the DA stage, the HEMS of each prosumer communicates the following information:

- Physical parameters of flexible loads and rooms. The parameters of the flexible loads are maximum changing and discharging power of the EV, maximum power of the TCL and efficiencies of the charging and discharging processes. The parameters of the rooms are estimated values of the thermal resistance and capacitance. These physical parameters can be provided by manufacturers or computed using estimation techniques [29].
- Scenarios of INL, dwelling active occupancy, EV and SL requirements. The EV and SL requirements define their flexibility, as well as the preferences of the prosumers. The methodologies used to generate the scenarios are described in ection 5.3.
- Temperature preferences specified by the prosumers. The preferences are temperature ranges. They define the flexibility of the TCL.

In the same period, the aggregator forecasts energy and imbalance prices, using the algorithms described in Section 5.5, and the weather service provider communicates scenarios of outdoor temperatures to the aggregator. Afterwards, the aggregator optimizes and submits the demand and supply bids to the DA energy market. This optimization procedure must occur between the 0th and 12th hours, as described in Fig. 1.

3.2. Description of the bidding optimization model

The aggregator defines demand and supply bids E_t^{DA} to submit to the DA energy market by solving the two-stage stochastic optimization model (5)–(19). The aim is to minimize the net cost of the aggregator buying and selling energy in DA and RT market stages. The objective function (5) has two terms:

1. The first term is the net cost of buying and selling energy E_t^{DA} at forecasted price $\hat{\lambda}_t^{DA,E}$ in the DA energy market. Positive values of E_t^{DA} are buying bids and negative values are selling bids;
2. The second term defines the expected imbalance cost, due to deviations between RT realizations and DA market commitments. Positive imbalance $I_{j,t}^{+}$(kWh) means surplus of generation $(I_t^{\wedge -} > 0)$ or shortage of demand $(I_t^{\vee} < 0)$. Negative imbalance $I_{j,t}^{-}$ means shortage of generation $(I_t^{\wedge -} < 0)$ or surplus of demand $(I_t^{\vee} > 0)$. Energy imbalances are valued at positive $\hat{\lambda}_t^{DA,+}$ and negative $\hat{\lambda}_t^{DA,-}$ forecasted imbalance prices;

The uncertainties are modeled through a set of scenarios $j \in S$ with probability of occurrence π_j. The bids are optimized along the optimization period H. Time intervals t of 1 h with length $\Delta t\,(h)$ are used, since market prices vary in an hourly basis.

$$Min \sum_{t\in H} (\hat{\lambda}_t^{DA,E} E_t^{DA} + \sum_{j\in S} \pi_j (\hat{\lambda}_t^{DA,-} I_{j,t}^{-} - \hat{\lambda}_t^{DA,+} I_{j,t}^{+})) \tag{5}$$

The market trading constraint (6) defines energy imbalances. Constraints (7) and (8) set the limits of the energy bids and imbalances. The maximum values $\overline{E}^{\wedge -}$ and $\overline{E}^{\vee}$ are defined, according to the contracted power for generation and demand of all prosumers.

$$I_{j,t}^{-} - I_{j,t}^{+} = E_{j,t}^{RT} - E_t^{DA}\,, \quad \forall\, j \in S, t \in H \tag{6}$$

$$-\overline{E}^{\wedge} \leqslant E_t^{DA} \leqslant \overline{E}^{\vee}\,, \quad \forall\, t \in H \tag{7}$$

$$0 \leqslant I_{j,t}^{+}, I_{j,t}^{-} \leqslant \max(\overline{E}^{\vee}, \overline{E}^{\wedge})\,, \quad \forall\, j \in S, t \in H \tag{8}$$

Constraint (9) sets the expected net load in RT equals to the sum of

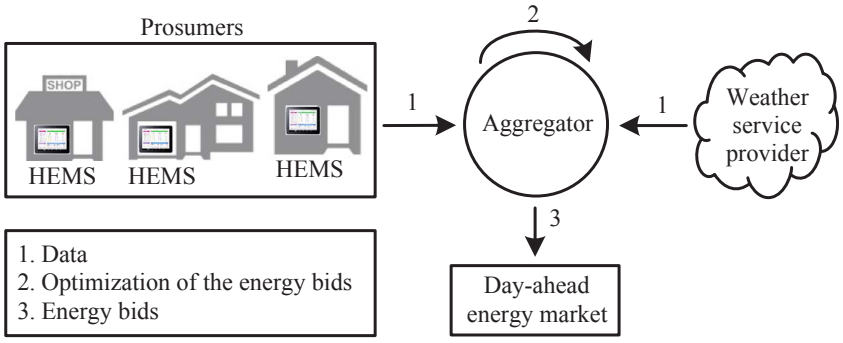

Fig. 3. System architecture and information chain in the DA stage.

INL and net consumption of the flexible loads. The electric power $P^{v}_{j,i,t}(kW)$ of load $i \in L^{v}$ is positive for demand and negative for generation.

$$E^{RT}_{j,t} = \sum_{v} \Big(\sum_{i \in L^{v}} P^{v}_{j,i,t}\Delta t\Big), \quad \begin{matrix} \forall\, j \in S, t \in H \\ v \in \{EV, TCL, SL, INL\} \end{matrix} \tag{9}$$

The complete formulation includes load constraints. The optimization of EV charging and discharging requires five constraints. Constraints (10) and (11) ensure that the charging $E^{EV,\vee}_{j,i,t}$ and discharging $E^{EV,\wedge-}_{j,i,t}$ energy do not exceed the maximum values of $\overline{P}^{EV,\vee}_{i}\Delta t$ and $\overline{P}^{EV,\wedge-}_{i}\Delta t$, respectively. The binary variable $\varnothing_{j,i,t}$ imposes one of the two constraints, i.e., it defines the mode of operation of the EV, charging or discharging. The net power of the EV is given by $P^{EV}_{j,i,t} = (E^{EV,\vee}_{j,i,t} - E^{EV,\wedge}_{j,i,t})/\Delta t$. Constraints (12) and (13) set the *SOC* (kWh) within its limits $[\underline{SOC}_{j,i}, \overline{SOC}_{j,i}]$. The parameters $\eta^{\vee}_{i}$ and $\eta^{\wedge-}_{i}$ are the efficiency of the charging and discharging processes. Constraint (14) sets the target *SOC* at departure time $t^{DE}_{j,i}$, and ensures that the preferences of the prosumers are satisfied. The preferences are represented by the parameters $t^{DE}_{j,i}$ and $SOC^{DE}_{j,i}$. The availability of the EV to charge and discharge is defined by $H^{EV}_{j,i}$. The scenario-based inputs related to the EV requirements are $\{t^{DE}_{j,i}, t^{AR}_{j,i}, SOC^{DE}_{j,i}, SOC^{AR}_{j,i}, H^{EV}_{j,i}, \ \forall\, j,i\}$.

$$0 \leqslant E^{EV,\vee}_{j,i,t} \leqslant \varnothing_{j,i,t}\overline{P}^{EV,\vee}_{i}\Delta t, \quad \forall\, j \in S, i \in L^{EV}, t \in H^{EV}_{j,i} \tag{10}$$

$$0 \leqslant E^{EV,\wedge}_{j,i,t} \leqslant (1-\varnothing_{j,i,t})\overline{P}^{EV,\wedge}_{i}\Delta t, \quad \forall\, j \in S, i \in L^{EV}, t \in H^{EV}_{j,i} \tag{11}$$

$$SOC_{j,i,t+1} = SOC_{j,i,t} + \eta^{\vee}_{i}E^{EV,\vee}_{j,i,t} - E^{EV,\wedge}_{j,i,t}/\eta^{\wedge}_{i}, \quad \forall\, j \in S, i \in L^{EV}, t \in H^{EV}_{j,i} \tag{12}$$

$$\underline{SOC}_{i} \leqslant SOC_{j,i,t+1} \leqslant \overline{SOC}_{i}, \quad \forall\, j \in S, i \in L^{EV}, t \in H^{EV}_{j,i} \tag{13}$$

$$SOC_{j,i,t^{DE}_{j,i}} = SOC^{DE}_{j,i}, \quad \forall\, j \in S, i \in L^{EV} \tag{14}$$

The TCL model adopted in this paper describes the operation of an inverter heat pump. However, the model can be adapted to another type of TCL. The optimization of TCL requires three constraints. Constraint (15) ensures that the electric power $P^{TCL}_{j,i,t}$ of the TCL does not exceed the maximum value of $\overline{P}^{TCL}_{i}$. The physically-based load equation (16) sets the temperature inside the room $\theta_{j,i,t+1}$ (°C) [11,16]. The parameters in (16) are thermal resistance R_i(°C/kW), capacitance C_i(kWh/°C) of the room, coefficient of performance COP_i and outdoor temperature $\theta^{0}_{j,t}$. Constraint (17) guarantees the preferences of the prosumers, when the room (or house) is occupied $O_{j,i}$. The preferences are an interval of temperatures predefined by the prosumer $[\underline{\theta}_i, \overline{\theta}_i]$. The scenario-based inputs are dwelling active occupancy and outdoor temperature $\{O_{j,i}, \theta^{0}_{j} \quad \forall\, j,i\}$.

$$0 \leqslant P^{TCL}_{j,i,t} \leqslant \overline{P}^{TCL}_{i}, \quad \forall\, j \in S, i \in L^{TCL}, t \in H^{TCL}_{i} \tag{15}$$

$$\theta_{j,i,t+1} = \beta_i\theta_{j,i,t} + (1-\beta_i)(\theta^{o}_{j,t} + COP_i \cdot R_i \cdot P^{TCL}_{j,i,t}), \beta_i = e^{-\frac{\Delta t}{C_i R_i}}, \quad \forall\, j \in S, i \in L^{TCL}, t \in H^{TCL}_{i} \tag{16}$$

$$\underline{\theta}_{i} \leqslant \theta_{j,i,t+1} \leqslant \overline{\theta}_{i}, \quad \forall\, j \in S, i \in L^{TCL}, t \in O_{j,i} \tag{17}$$

The scheduling of SL requires two constraints. Constraint (18) defines the electric power $P^{SL}_{j,i,t}$ imposed by the power profile $Pr^{SL}_{j,i,w}$. The binary variable $\psi_{j,i,t}$ schedules the beginning of a working cycle of duration $D_{j,i}$. Constraint (19) ensures that one working cycle is started at each availability period $\underline{H}^{SL}_{j,i}$. The scenario-based inputs related to the SL requirements are availability period to complete a working cycle, power profile, availability to start a working cycle and number of time intervals of a working cycle $\{\overline{H}^{SL}_{j,i}, Pr^{SL}_{j,i}, \underline{H}^{SL}_{j,i}, D_{j,i}, \ \forall\, j,i\}$. The availability period to complete a working cycle defines the preferences of the prosumers.

$$P^{SL}_{j,i,t} = \sum_{w=0}^{D_{j,i}-1} Pr^{SL}_{j,i,w}\psi_{j,i,t-w}, \quad \forall\, j \in S, i \in L^{SL}, t \in \overline{H}^{SL}_{j,i} \tag{18}$$

$$\sum_{t \in \underline{H}^{SL}_{j,i}} \psi_{j,i,t} = 1, \quad \forall\, j \in S, \quad \forall\, i \in L^{SL} \tag{19}$$

The uncertainty of the INL is modeled through scenarios of power profiles $\{Pr^{INL}_{j,i}, \ \forall\, j,i\}$. The electric power of the INL is given by $P^{INL}_{j,i,t} = Pr^{INL}_{j,i,t}$.

4. Real-time optimization

4.1. System architecture and information chain

During the operating day, the aggregator sets the operation of the flexible loads using a MPC method [30,31]. The aim is to control the aggregated net consumption of the flexible loads, in order to minimize the net cost of the aggregator buying and selling energy in RT. The sequential steps of the proposed MPC method are illustrated in Fig. 4 and described below:

1. At the beginning of each time interval t, the following parameters are communicated and updated by the HEMS of each prosumer: TCL – temperature of the room θ_i and dwelling occupancy O_i defined by the user or forecasted by the HEMS; INL – forecasted power profile $\hat{P}r^{INL}_{i}$; EV – SOC of the plugged EV and information from the recently plugged EV, such as actual SOC, departure time t^{DE}_{i} and desired SOC at t^{DE}_{i}; SL – information about the working cycles (state of the cycle, power profile Pr^{SL}_{i} availability to start $\underline{H}^{SL}_{i}$ and finish $\overline{H}^{SL}_{i}$). The weather service provider communicates updated forecasts of outdoor temperature $\hat{\theta}^{o}_{t}$, if available;
2. The aggregator dispatches the flexible loads by solving the deterministic optimization model described in Section 4.2 with this new information. The aggregator forecasts new imbalance prices, if new market information is available.
3. Power (EV) and temperature (TCL) set-points, as well as start orders (SL) are communicated by the aggregator to the HEMS, which conveys the set-points to the appliances; this sequential process is repeated for the next time interval, $t + 1$ (go to step 1).

The MPC method runs in continuous mode during the operation day in cycles of 15 min. The SL and EV are initially scheduled, when the users define their preferences and turn on the appliances. The TCL are scheduled in continuous mode. The dispatch of the flexible loads takes into account the uncertainty of the INL and outdoor temperatures through point forecasts. All the other load parameters are perfectly known.

4.2. Formulation of the deterministic optimization problem of the model predictive control method

The deterministic optimization problem is formulated with the objective of minimizing the net cost of the aggregator in RT. The objective

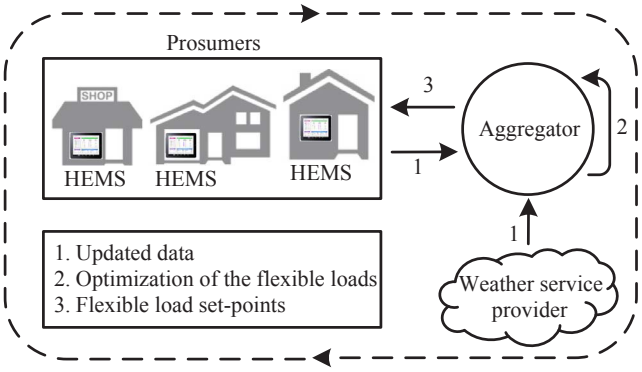

Fig. 4. System architecture and information chain in the RT stage.

function (20) has three terms. The first term is the cost and revenue of buying and selling energy $E^{RT}_{t+k|t} E^{RT}_{t+k|t} E^{RT} t + kt$ at energy clearing price $\lambda^{RT,E}_{t+k|t}$. The second and third terms are the regulation costs for negative $I^{-}_{t+k|t}$ and positive $I^{+}_{t+k|t}$ energy imbalances. The imbalance prices $\hat{\lambda}^{RT,-}_{t+k|t}$ and $\hat{\lambda}^{RT,+}_{t+k|t}$ are point forecasts predicted in RT stage. Time intervals t and k of 15 min (Δk) are considered.

$$Min \sum_{k \in H} \begin{pmatrix} \lambda^{RT,E}_{t+k|t} E^{RT}_{t+k|t} + (\hat{\lambda}^{RT,-}_{t+k|t} - \lambda^{RT,E}_{t+k|t}) \cdot I^{-}_{t+k|t} \\ + (\lambda^{RT,E}_{t+k|t} - \hat{\lambda}^{RT,+}_{t+k|t}) \cdot I^{+}_{t+k|t} \end{pmatrix} \quad (20)$$

The market trading constraint (21) sets the energy imbalances and constraint (22) defines their limits. In the RT stage, the energy bids $E^{DA}_{t+k|t}$ are values resulting from the DA optimization, instead of decision variables.

$$I^{-}_{t+k|t} - I^{+}_{t+k|t} = E^{RT}_{t+k|t} - E^{DA}_{t+k|t}, \quad \forall\, k \in H \quad (21)$$

$$0 \leqslant I^{+}_{t+k|t}, I^{-}_{t+k|t} \leqslant \max(\overline{E}^{\vee}, \overline{E}^{\wedge}), \quad \forall\, k \in H \quad (22)$$

Constraint (23) sets the RT net load of all prosumers' resources. The electric power $P^{v}_{i,t+k|t}$ is positive for demand and negative for generation.

$$E^{RT}_{t+k|t} = \sum_{v} \left(\sum_{i \in L^{v}} P^{v}_{i,t+k|t} \Delta k \right), \quad \begin{matrix} \forall\, k \in H \\ v \in \{EV, TCL, SL, INL\} \end{matrix} \quad (23)$$

Constraint (24) sets the limits of the net load of each prosumer y, based on their contracted power of consumption $CP^{\vee}_{y}(kW)$ and generation $CP^{\wedge -}_{y}$.

$$-CP^{\wedge}_{y} \leqslant \sum_{v} \sum_{i \in L^{v}_{y}} P^{v}_{i,t+k|t} \leqslant CP^{\vee}_{y}, \quad \begin{matrix} \forall\, y \in N, k \in H \\ v \in \{EV, TCL, SL, INL\} \end{matrix} \quad (24)$$

The optimization of EV charging and discharging requires five constraints. Constraints (25) and (26) define if the EV charges or discharges. Constraints (27) and (28) set the SOC within its limits. Constraint (29) sets the SOC at departure time and ensures the preferences of the prosumers.

$$0 \leqslant E^{EV,\vee}_{i,t+k|t} \leqslant \varnothing_{i,t+k|t} \overline{P}^{EV,\vee}_{i} \Delta k, \quad \forall\, i \in L^{EV}, k \in H^{EV}_{i} \quad (25)$$

$$0 \leqslant E^{EV,\wedge}_{i,t+k|t} \leqslant (1 - \varnothing_{i,t+k|t}) \overline{P}^{EV,\wedge}_{i} \Delta k, \quad \forall\, i \in L^{EV}, k \in H^{EV}_{i} \quad (26)$$

$$SOC_{i,t+k+1|t} = SOC_{i,t+k|t} + E^{EV,\vee}_{i,t+k|t} \eta^{\vee}_{i} - E^{EV,\wedge}_{i,t+k|t} / \eta^{\wedge}_{i}, \quad \forall\, i \in L^{EV}, k \in H^{EV}_{i} \quad (27)$$

$$\underline{SOC}_{i} \leqslant SOC_{i,t+k+1|t} \leqslant \overline{SOC}_{i}, \quad \forall\, i \in L^{EV}, k \in H^{EV}_{i} \quad (28)$$

$$SOC_{i,t^{DE}_{i}} = SOC^{DE}_{i}, \quad \forall\, i \in L^{EV}, k \in H^{EV}_{i} \quad (29)$$

The scheduling of TCL requires three constraints. Constraint (30) ensures the power limits of the TCL. Constraint (31) sets the temperature inside the room. Constraint (32) ensures the preferences of the prosumers, when the home/room is occupied.

$$0 \leqslant P^{TCL}_{i,t+k|t} \leqslant \overline{P}^{TCL}_{i}, \quad \forall\, i \in L^{TCL}, k \in H^{TCL}_{i} \quad (30)$$

$$\theta_{i,t+k+1|t} = \beta_i \theta_{i,t+k|t} + \left(1 - \beta_i\right)\left(\hat{\theta}^{o}_{t+k|t} + COP_i \cdot R_i \cdot P^{TCL}_{i,t+k|t}\right),$$
$$\beta_i = e^{-\frac{\Delta k}{C_i R_i}}, \quad \forall\, i \in L^{TCL}, k \in H^{TCL}_{i} \quad (31)$$

$$\underline{\theta}_{i} \leqslant \theta_{i,t+k+1|t} \leqslant \overline{\theta}_{i}, \quad \forall\, i \in L^{TCL}, k \in O_i \quad (32)$$

The scheduling of SL requires two constraints. Constraint (33) sets the electric power. Constraint (34) ensures that the working cycle is started within the availability period $\underline{H}^{SL}_{i}$. The availability period to complete a working cycle $\overline{H}^{SL}_{i}$ defines the preferences of the prosumers. The INL is given by $P^{INL}_{i,t+k|t} = \hat{P} r^{INL}_{i,t+k|t}$.

$$P^{SL}_{i,t+k|t} = \sum_{w=0}^{D_i - 1} Pr^{SL}_{i,w} \psi_{i,t+k-w|t}, \quad \forall\, i \in L^{SL}, k \in \overline{H}^{SL}_{i} \quad (33)$$

Table 1
Physical parameters of the TCL and rooms.

R (°C/kW)	C (kWh/°C)	COP	$\overline{P}$
6.7–50.1	0.5–3.6	4.6–4.8	0.9–1.25

$$\sum_{k \in \underline{H}^{SL}_{i}} \psi_{i,t+k|t} = 1, \quad \forall\, i \in L^{SL} \quad (34)$$

5. Case study

5.1. Short Description

The aggregator of small prosumers participates in the energy market of MIBEL. The prosumers are from Porto (Portugal) and the analyzed period corresponds to the first week of December 2015. The aggregator manages 1000 small prosumers characterized by 1000 PV systems and 3000 flexible loads. Each prosumer has 1 PV system and three flexible loads (1 EV, 1 TCL and 1 SL). The contracted power of each prosumer is 13.8 kVA.

5.2. Physical parameters of thermostatically controlled loads and electric vehicles

The parameters of the TCL and rooms are presented in Table 1. The room parameters R and C were computed, based on physical characteristics of Portuguese buildings. The parameters of the TCL (COP and $\overline{P}^{TCL}$) were collected from 10 manufactures (e.g., [32]). The physical parameters were randomly selected. The intervals of thermal flexibility $[\underline{\theta}, \overline{\theta}]$ were randomly selected between 19 and 23 °C.

The discharging and charging power rates of the EV ($\overline{P}^{EV}$) were randomly selected by choosing one of the two values 3.7 or 7 kW. The efficiency of the charging $\eta^{\vee}$ and discharging $\eta^{\wedge -}$ processes is 0.93.

5.3. Generation of scenarios

Twenty scenarios with equal probability of occurrence π_j were computed, based on scenarios of outdoor temperature $\{\theta^{0}_{j}, \ \forall\, j\}$, dwelling active occupancy $\{O_{j,i}, \ \forall\, j,i\}$, EV requirements $\{t^{DE}_{j,i}, t^{AR}_{j,i}, SOC^{DE}_{j,i}, SOC^{AR}_{j,i}, H^{EV}_{j,i}, \ \forall\, j,i\}$, INL $\{Pr^{INL}_{j,i}, \ \forall\, j,i\}$ and SL requirements $\{\overline{H}^{SL}_{j,i}, Pr^{SL}_{j,i}, \underline{H}^{SL}_{j,i}, D_{j,i}, \ \forall\, j,i\}$. Depending of the adopted framework, the scenarios may be generated by the aggregator or HEMS.

5.3.1. Dwelling active occupancy

The scenarios of dwelling active occupancy were generated, based on daily routines of Portuguese families. Typically, a Portuguese family leaves home to go to work at 8th hour and arrives at home at 20th hour.

5.3.2. Outdoor temperature

The scenarios of outdoor temperature were generated using the Gaussian copula method (described in [33,34]). The probabilistic forecasts were produced by the quantile regression method using forecasted outdoor temperature as explanatory variable (available in [35]). Fig. 5 shows an example of twenty scenarios of outdoor temperature for November 30th in Porto.

5.3.3. Electric vehicle requirements

The EV requirements consists of four parameters: departure t^{DE} and arrival t^{AR} times, SOC at arrival time (SOC^{AR}) and desired SOC at departure time (SOC^{DE}). The availability of the EV to charge and discharge is defined by the period between the arrival and departure times (H^{EV}).

The synthetic annual time series of EV driving patterns were generated by a discrete-time-space Markov chain. More detailed

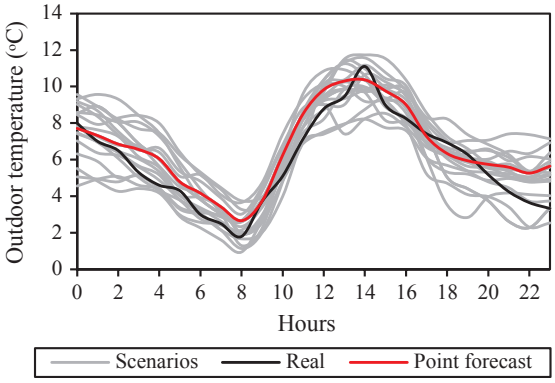

Fig. 5. Twenty scenarios of outdoor temperature for November 30th, 2015 (Porto).

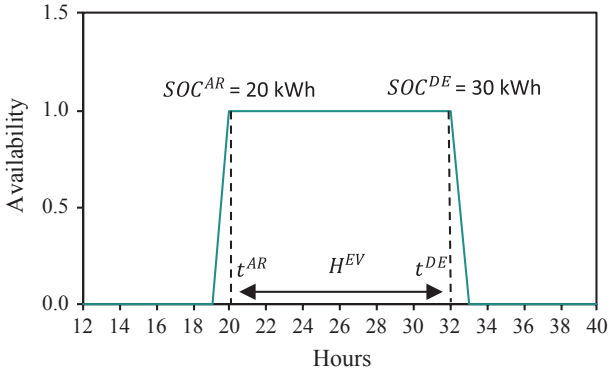

Fig. 6. One scenario of EV requirements.

information about the methodology and the generated time series can be found in [36,37]. Based on the generated time series, scenarios of EV requirements were computed by a seasonal naïve forecasting algorithm. Fig. 6 shows one scenario of EV requirements. The EV is plugged-in when the availability is equal to one.

5.3.4. Inflexible net load

The scenarios of INL were generated by the Gaussian copula method. The probabilistic forecasts were produced by the quantile regression method using time of the day and season as explanatory variables. The past observations of INL were defined based on load and microgeneration profiles available in the website of the Portuguese transmission system operator [38] and energy regulator [39]. Fig. 7 shows an example of twenty scenarios of INL for November 30th in Porto (one prosumer).

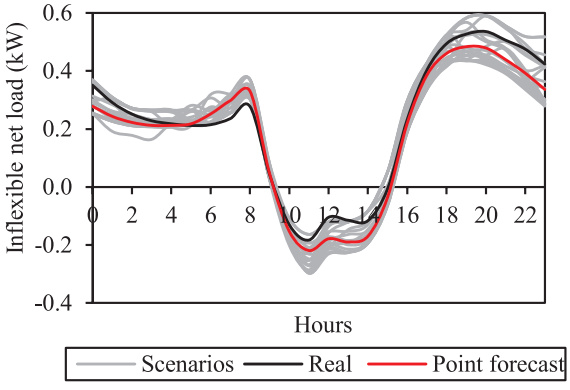

Fig. 7. Twenty scenarios of INL for November 30th, 2015 (one prosumer).

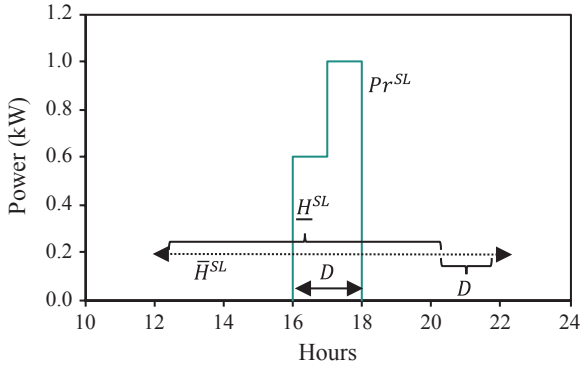

Fig. 8. One scenario of SL requirements.

5.3.5. Shiftable load requirements

The SL requirements consist of two parameters (Pr^{SL},D) and two sets of time intervals ($\overline{H}^{SL}$,$\underline{H}^{SL}$). The scenarios of SL requirements were computed by a seasonal naïve forecasting algorithm. The inputs are synthetic annual time series of SL requirements. Fig. 8 shows one scenario of SL requirements.

The synthetic annual time series of SL requirements were generated by a three-step approach. Firstly, the start time of the events (or working cycles) for one year were determined by a cumulative distribution function available in [40]. Secondly, the power profile of the events Pr^{SL} and the respective durations D were defined, based on values randomly selected from intervals of [0.2, 2] kW and [2,8] time slots of 15 min [41]. Thirdly, the availability periods to start ($\underline{H}^{SL}$) and complete ($\overline{H}^{SL}$) the working cycles were computed. Periods between 4 and 8 h were used to set $\underline{H}^{SL}$. The $\overline{H}^{SL}$ was defined based on D and $\underline{H}^{SL}$ ($\underline{H}^{SL} \subset \overline{H}^{SL}$).

5.4. Information in the real-time stage

The EV and SL requirements were computed based on the generated time series. For simplification purposes, real values of INL and outdoor temperatures were considered.

5.5. Forecasting of electricity prices

The DA and RT optimization procedures consider two type of prices: MIBEL energy prices and Portuguese imbalance prices. The energy prices only assume non-negative values. The imbalance prices can assume positive and negative values.

The DA optimization uses as inputs forecasts of energy and imbalance prices ($\hat{\lambda}_t^{DA,E}$,$\hat{\lambda}_t^{DA,-}$,$\hat{\lambda}_t^{DA,+}$). The electricity prices were forecasted for a time horizon of 48 h ahead using the gradient boosting algorithm [42] from the python package “scikit-learn” [43]. The following explanatory variables were used: energy prices – forecasted demand, wind and solar generation of the Iberian Peninsula and time of the day; imbalance prices – forecasted demand, wind and solar generation of the Portuguese control area, forecasted energy price and time of the day.

The RT optimization uses as inputs energy clearing prices and forecasted imbalance prices ($\lambda_t^{RT,E}$,$\hat{\lambda}_t^{RT,-}$,$\hat{\lambda}_t^{RT,+}$). The imbalance prices were forecasted for a time horizon of 24 h ahead using the gradient boosting algorithm and the following explanatory variables: clearing energy prices; forecasted demand, wind and solar generation of the Portuguese control area; and time of the day.

One year of market data (2015) collected from the ENTSO-E website [44] was used to forecast the MIBEL energy prices and the Portuguese imbalances prices. Table 2 shows the average values of the mean absolute error (MAE) and spearman’s rank correlation [45] for the first week of December 2015.

Table 2
MAE and spearman's correlation of forecasted electricity prices.

	$\hat{\lambda}_t^{DA,E}$	$\hat{\lambda}_t^{DA,-}$	$\hat{\lambda}_t^{DA,+}$	$\hat{\lambda}_t^{RT,-}$	$\hat{\lambda}_t^{RT,+}$
MAE (€/MWh)	3.1	8.6	8.3	7.2	8.5
Spearman's correlation	0.90	0.55	0.43	0.57	0.49

5.6. Benchmarks

The proposed DA bidding and RT control strategies are compared to other theoretical benchmark approaches in Section 6. Four DA bidding strategies are analyzed.

Table 3 compares the main characteristics of the bidding strategies. Perfect and deterministic strategies optimize the energy bids in order to minimize the net costs of buying and selling energy in the DA market. They adopt deterministic models similar to the approaches described in [5–7,10]. The only difference between these two strategies is the input data. Perfect strategy uses perfectly forecasted information (i.e., price and load parameters), whereas deterministic strategy considers point forecasted information (or one single scenario). The smart strategy optimizes the bids with the aim of minimizing the net cost of buying and selling energy in the DA and RT market stages and models the load uncertainty through multiple scenarios. The inflexible strategy does not optimize the flexibility of the prosumers, i.e., considers that all net load is inflexible. Typically, this is the strategy adopted by retailers.

Two RT control strategies are analyzed. Table 4 compares the main characteristics of the RT control strategies. Both strategies consider the MPC method described in Section 4.1. The different between smart and flexible strategies is the objective function of the deterministic optimization model. The smart strategy aims to minimize the net cost of the aggregator buying and selling energy in RT, while flexible strategy aims to minimize RT energy imbalances. The smart strategy requires the forecasting of imbalance prices in RT. The flexible strategy emulates the direct load control methods [14–17], whose objective is to deliver products traded in the DA markets.

The DA bidding strategies are compared in Section 6.1, while RT control strategies are compared in Section 6.2. Additionally, a comparison between combinations of DA and RT strategies is made in Section 6.3. Table 5 presents the combined strategies that are compared.

6. Results

6.1. Comparison between day-ahead bidding strategies

6.1.1. Daily day-ahead bidding results

Fig. 9 illustrates the supply and demand bids of smart, deterministic and inflexible strategies for November 30th (Monday). Positive values are demand bids and negative values are supply bids. As shown, the "inflexible" demand bids are placed in hours of high energy prices. On the other hand, with optimized strategies (perfect, smart and deterministic), the demand bids are mostly placed in hours of low energy prices and supply bids in hours of high energy prices. Between the 10th and 14th hours, the aggregator submits bids on the supply side of the market, because it corresponds to the time of the day with the highest forecasted PV generation. At night, the supply bids result from EV featuring vehicle-to-grid.

The smart strategy introduces one additional term compared to the deterministic strategy, the sensitivity to imbalance costs, which affects the definition of the bids. In the 1st hour, the demand bid placed by smart strategy is slightly lower than by deterministic strategy. This placement is due to the penalty price for positive load imbalances ($\lambda_t^- - \lambda_t^E = 11.1$ €/MWh), which is lower than for negative load imbalances ($\lambda_t^E - \lambda_t^+ = 12.0$ €/MWh). This means that is more advantageous for the aggregator to present a short demand position than a long position in the 1st hour. A similar type of reasoning can be applied to the supply side, based on the generation imbalance mechanism described by Eq. (2).

6.1.2. Weekly day-ahead bidding results

Table 6. compares the cumulative DA bidding results obtained from perfect, smart, deterministic and inflexible strategies for the first week of December 2015. The deterministic strategy presents the lowest bidding net cost (6.43 k€) followed by smart, perfect and inflexible strategies (6.46, 7.06 and 7.93 k€). However, it should be noted that the overall performance of the bidding strategies can only be effectively assessed in RT, due to the uncertainties of electricity prices and net consumption. This assessment is made in Section 6.3.

The smart strategy shows a conservative behavior during the first week of December, since it has a positive expected imbalance cost of 0.05 k€. The imbalance cost is due to the positive difference between expected net load and net bids ($I^- = 0.34$ MWh). This means that it is more profitable for the aggregator to present a short position. Fig. 10 demonstrates the conservative behavior of the smart strategy. The smart strategy places lower quantities of demand and supply bids than the deterministic strategy almost all days. This behavior is due to two reasons:

- The stochastic nature of the optimization model adopted by the smart strategy, which incorporates the uncertainty of the net consumption through multiple scenarios;
- The imbalance cost term in the objective function, which values the uncertainty of the net consumption.

The inflexible strategy places low quantities of supply bids, since it does not exploit the flexibility of the EV to store and inject energy into the grid.

Table 3
Main characteristics of the four DA bidding strategies.

	Optimization model	Load uncertainty	Price uncertainty
Smart	Two-stage stochastic optimization model described in Section 3.2	Multiple scenarios	Point forecasts
Deterministic	Deterministic optimization model with the objective function $Min \sum_{t\in H} \hat{\lambda}_t^{DA,E} E_t^{DA}$ (35) subject to $E_t^{DA} = \sum_v (\sum_{i\in L^v} P_{0,i,t}^v \Delta t)$ and (10)–(19)	Point forecasts (or one scenario $\Rightarrow j = 0$)	Point forecasts
Perfect	Optimization model adopted by the deterministic strategy	Perfect forecasts	Perfect forecasts
Inflexible[a]	No optimization	Point forecasts	Not considered

[a] It is also considered in RT.

Table 4
Main characteristics of the two RT control strategies.

	Optimization model of the MPC method	Load uncertainty	Price uncertainty
Smart	Deterministic optimization model described in ection 4.2	Real data and point forecasts	Point forecasts of imbalance prices and energy clearing prices
Flexible	Deterministic optimization model with the objective function $Min \sum_{k\in H} I^{-}_{t+k\|t} + I^{+}_{t+k\|t}$ (36) subject to (21)–(34)	Real data and point forecasts	No prices are considered

Table 5
Combined DA and RT strategies.

Name	Perfect	Smart_1	Smart_2	Deter_1	Deter_2	Inflexible
DA bidding strategy	Perfect	Smart	Smart	Deterministic	Deterministic	Inflexible
RT control strategy	–	Smart	Flexible	Smart	Flexible	Inflexible

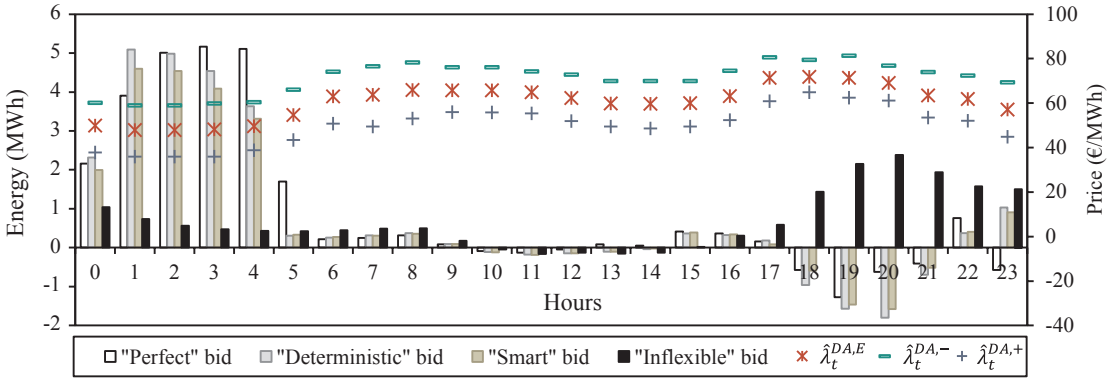

Fig. 9. Demand and supply bids obtained from perfect, smart, deterministic and inflexible strategies for November 30th (Monday). The positive values are demand bids and the negative values are supply bids.

Table 6
Cumulative DA bidding results obtained from perfect, smart, deterministic and inflexible strategies for the first week of December 2015.

	Perfect	Smart	Deterministic	Inflexible
Net cost (k€)	7.06	6.46	6.43	7.93
Energy cost (k€)	9.09	8.62	9.16	8.06
Energy revenue (k€)	2.03	2.21	2.73	0.13
Expected imbalance cost (k€)	–	0.05	–	–
Demand bids (MWh)	174.50	168.59	180.07	132.76
Supply bids (MWh)	30.36	33.88	42.15	2.17
Expected net load (MWh)	–	135.04	–	–

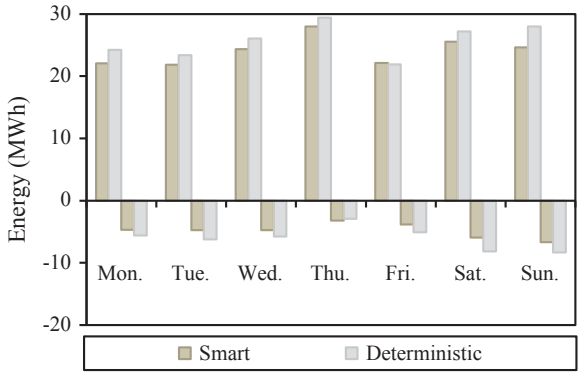

Fig. 10. Cumulative supply and demand bids of smart and deterministic strategies for the first week of December 2015.The positive values are demand bids and the negative values are supply bids.

6.2. Comparison between real-time control strategies

6.2.1. Daily real-time results

Fig. 11 compares the energy imbalances computed through smart and flexible control strategies for November 30st (Monday). The energy imbalances were computed based on the energy bids defined by the DA smart strategy (in Section 6.1.1). The positive values are positive imbalances and the negative values are negative imbalances.

The smart strategy optimizes the net consumption of the aggregated flexible loads, based on energy clearing prices and forecasted imbalance prices. This means that the smart strategy may deviate from DA bids in time intervals of low prices, if it is profitable. One example of this behavior is the 4th hour, where the aggregator increases consumption. The flexible strategy minimizes the energy imbalances without considering their economic value. The period between 6th and 9th hours represents this behavior, since flexible strategy increases the net consumption in hours of high prices. However, smart and flexible strategies may present similar behaviors, when the flexibility of the prosumers is limited, as shown in the period between 17th and 19th hours.

6.2.2. Weekly real-time results

Table 7 compares the cumulative RT results obtained from smart and flexible strategies for the first week of December 2015. The smart strategy presents lower net cost (7.41 k€) than flexible strategy (7.72 k €). However, it presents the highest regulation cost (0.36 k€). This shows that smart strategy arbitrages to reduce the total net cost of the aggregator. The flexible strategy generally presents low imbalances, since its main objective is to minimize energy imbalances.

Fig. 12 compares the cumulative RT net cost and net consumption of smart and flexible strategies along the week. The smart strategy outperforms or equals flexible strategy every day, even when it presents

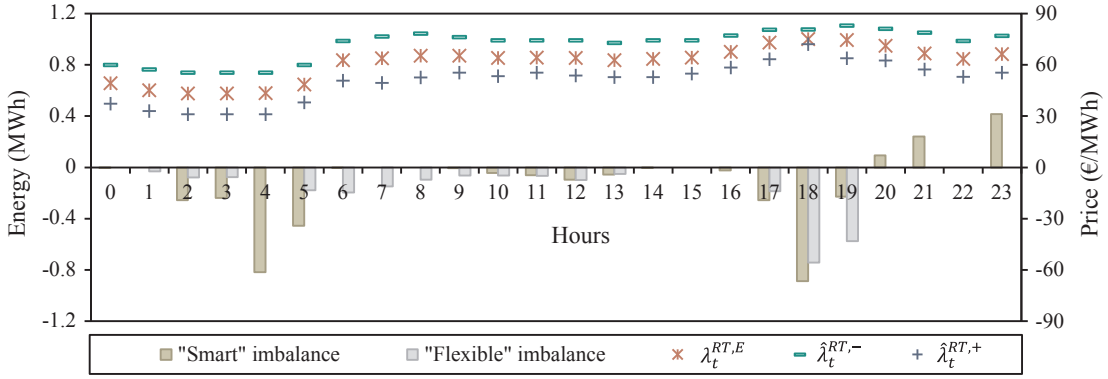

Fig. 11. Positive and negative imbalances obtained from smart and flexible strategies for November 30th (Monday). The positive values are positive imbalances and the negative values are negative imbalances.

Table 7
Cumulative RT results obtained from smart and flexible strategies for the first week of December 2015.

	Smart	Flexible
Net cost (k€)	7.41	7.72
Energy cost (k€)	9.05	9.10
Energy revenue (k€)	2.00	1.59
Regulation cost (k€)	0.36	0.21
Net load (MWh)	142.69	147.58
Energy imbalance (MWh)	22.19	13.06

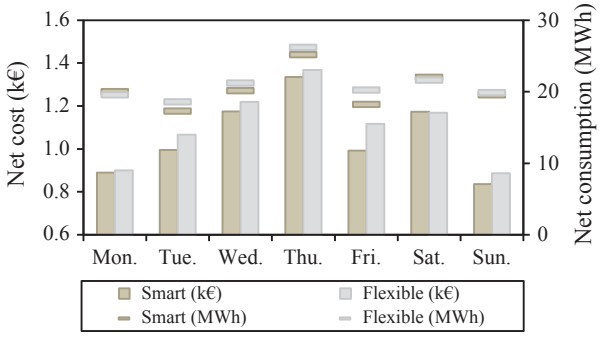

Fig. 12. Cumulative RT net cost and net consumption of smart and flexible strategies for the first week of December 2015.

Table 8
Cumulative RT results obtained from six combined strategies for the first week of December 2015.

Combined strategy	Perfect	Smart_1	Deter_1	Smart_2	Deter_2	Inflexible
DA strategy	Perfect	Smart	Deter.	Smart	Deter.	Inflexible
RT strategy	–	Smart	Smart	Flexible	Flexible	Inflexible
Net cost (k€)	7.07	7.41	7.59	7.72	7.95	8.60
Energy cost (k€)	9.09	9.05	9.14	9.10	9.32	8.51
Energy revenue (k€)	2.02	2.00	2.07	1.59	1.76	0.09
Regulation cost (k€)	0.00	0.36	0.52	0.21	0.39	0.18
Load (MWh)	174.50	172.47	174.70	171.56	175.85	134.38
Generation (MWh)	30.36	29.78	30.89	23.99	26.60	1.39

similar values of net consumption (e.g., Monday and Sunday). The daily net costs follow the same trend of the weekly net costs. Therefore, it is more beneficial for the aggregator to use always the smart strategy. The only situation where the adoption of the flexible strategy would make sense is when the aggregator does not have access to the electricity prices. However, this is a very unlikely scenario.

6.3. Comparison between combined day-ahead and real-time strategies

Table 8 presents the cumulative RT results of six combined strategies for one week. The perfect strategy presents the lowest net cost (7.07 k€), as expected, since it considers perfect information. However, perfect forecasts will never be possible due to the uncertain nature of the optimization input information. Therefore, this result should be interpreted, as the minimum theoretical net cost that the aggregator can obtain.

Under uncertainty conditions, smart_1 strategy presents the lowest net cost (7.41 k€). Both smart strategies (1 and 2) outperform the respective deterministic strategies. The cost term that experienced the highest reduction with the adoption of smart strategies was the regulation term, which was reduced by 30.7% (0.16 k€) and 45.8% (0.18 k €), when compared to the respective deterministic strategies. This proves that the proposed two-stage stochastic model provides a better bidding strategy than deterministic models. The RT smart strategy outperforms flexible strategy by reducing the net cost of smart_1 and deter_1 strategies in 3.9% (0.30 k€) and 4.4% (0.35 k€), when compared to smart_2 and deter_2 strategies. Therefore, RT arbitrage reduces the net cost of the aggregator. The margin for improvement of smart_1 is small (4.7%, 0.35 k€), based on the results of the perfect strategy. However, it is still possible to increase its performance by improving the electricity prices forecasting and the modeling of net load uncertainty.

Fig. 13 compares the cumulative RT net cost and consumption of six combined strategies for the first week of December 2015. The daily net costs follow the same trend of the weekly net costs described in Table 8. The optimized strategies outperform inflexible strategy every day, even when they present higher net consumption. Perfect strategy presents higher net cost than smart_1 strategy on Monday and Saturday, because of the higher net consumption. The difference of net consumption between strategies is mainly due to the inter-day trading behavior of the EV.

The adoption of optimized strategies reduces the net cost of the aggregator. In comparison with the inflexible approach, the maximum weekly savings under uncertainty conditions is 1.19 k€ with smart_1 (13.8%). The aggregator may keep part of the savings as profits and use the other part to remunerate the flexibility provided by its clients. The aggregator can remunerate the flexibility of the clients by offering cheaper retailing tariffs or a discount in the monthly electricity bill.

6.4. Evaluation of a different mix of distributed energy resources

The proposed case study consists of 1000 small prosumers from MIBEL. The first scenario of distributed energy resources analyzed is characterized by 1000 PV systems and 3000 flexible loads (1000 EV, 1000 TCL and 1000 SL), as described in Section 5.1. To demonstrate the effectiveness and replicability of the proposed strategies, another

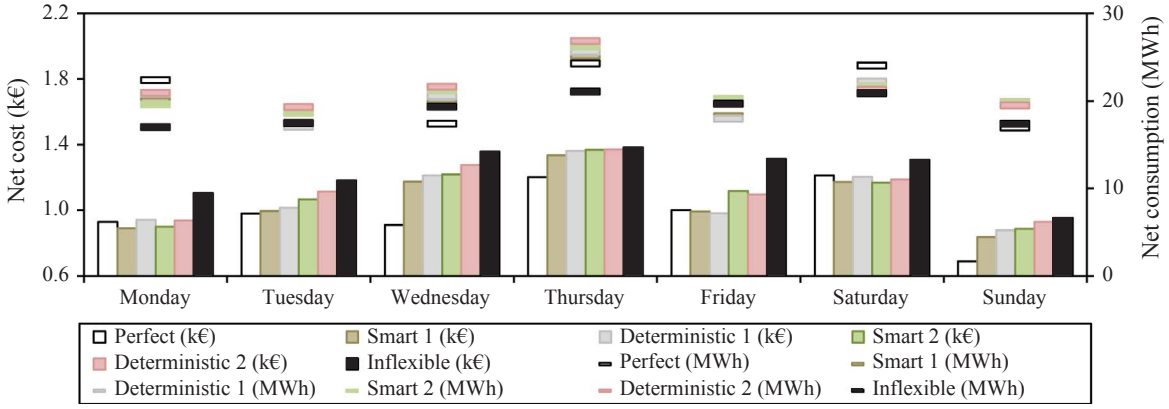

Fig. 13. Cumulative RT net cost and consumption obtained from six combined strategies for the first week of December 2015.

Table 9
Cumulative DA and RT net costs obtained from six combined strategies for the first week of December of 2015 and for the second scenario of distributed energy resources.

Combined strategy	Perfect	Smart_1	Deter_1	Smart_2	Deter_2	Inflexible
DA strategy	Perfect	Smart	Deter.	Smart	Deter.	Inflexible
RT strategy	–	Smart	Smart	Flexible	Flexible	Inflexible
DA net cost (k€)	5.62	5.25	5.21	5.25	5.21	6.24
RT net cost (k€)	5.62	5.80	5.91	5.95	6.05	6.72

Table 10
Problem size and execution time of the DA and RT optimizations (average values).

	DA smart	DA deterministic	RT smart	RT flexible
Continuous variables	1,816,042	93,649	91,793	91,733
Binary variables	304,146	16,212	15,118	15,077
Constraints	2,728,824	141,119	143,004	142,941
Execution time	6.3 min	3.1 s	4.6 s	2.6 min

scenario of distributed energy resources is analyzed in this section. This second scenario consists of 700 PV systems and 1300 flexible loads (600 EV, 400 TCL and 300 SL).

Table 9 shows the cumulative DA and RT net costs of the six combined strategies for the first week of December of 2015 and for the second scenario of distributed energy resources. Perfect strategy outperforms the other strategies with the lowest RT net cost of 5.62 k€. Under uncertainty conditions, smart_1 presents the lowest RT net cost of 5.25 k€. The net costs of the second scenario are lower than the net costs of the first scenario due to the lower number of distributed energy resources considered. The DA and RT net costs of both scenarios present the same order in terms of profit (see Tables 6 and 8). This demonstrates the effectiveness and replicability potential of the proposed strategies.

The maximum weekly savings under uncertainty conditions is 0.92 k€ with smart_1 strategy (13.7%), when inflexible approach is used as benchmark. The difference of cost savings with smart_1 between the first and second scenarios is 0.27 k€, which corresponds to a decrease of 22.7%. This shows that exploiting the flexibility of a higher number of distributed energy resources may increase the profits (i.e., savings) of the aggregator. Therefore, it may be beneficial for the aggregator to transform a large share of the savings into economic incentives for the customers, in order to attract more clients.

6.5. Computational performance

The optimization problems were solved using the python API of IBM ILOG CPLEX™ 12.7 solver on a 64-bit MS Windows©2008 Server machine with 96 GB RAM and an Intel© Xeon™ E-5680 CPU clocked at 3.33 GHz.

The problem size and execution time of the DA and RT optimizations are presented in Table 10. They result from solving the case study described in Section 5.1. The numerical results show suitable execution times for the market timeline. The computation time of the two-stage stochastic optimization model (DA smart) can be further reduced, if scenario reduction techniques are applied [46]. However, this issue is not in the scope of this paper.

7. Conclusions

The expected transformation of small consumers into prosumers, together with the deployment of smart home technologies, represents an opportunity for an aggregator to trade prosumers' flexibility in the energy market. At the same time, it gives the chance to prosumers value their flexibility and excess of generation without relying on storage technologies. To enable these new activities of the aggregator, two optimization procedures were proposed in this work: a two-stage stochastic optimization model to define demand and supply bids and a MPC method to control aggregated flexible loads in RT.

Under uncertainty conditions, the proposed strategies (named smart) outperform other theoretical benchmarks, such as deterministic, flexible and inflexible approaches. The two-stage stochastic optimization model increases the robustness of the energy bids by incorporating the uncertainty of flexible and INL in the optimization process. This reduces the net cost of the aggregator, namely the regulation costs. The proposed MPC method enables energy arbitrage in RT, which contributes to mitigate DA forecasting errors and to reduce the net cost of the aggregator. The numerical results show that smart_1 strategy reduces the net cost of the aggregator in average in 14%, when compared to a typical strategy used by retailers (inflexible strategy). Furthermore, the results also show that managing a higher number of distributed energy resources contributes to increase the savings (i.e., profits) of the aggregator. Therefore, it may be beneficial for the aggregator to transfer a large share of the savings to the prosumers (i.e., pay more for the flexibility provided by the customers), in order to attract more clients.

Future work will focus on developing new optimization models to support the participation of an aggregator of small prosumers in multiple market sessions, such as energy and reserves. Furthermore, remuneration mechanisms will be investigated too.

Acknowledgments

The work of José Iria was supported by Fundação para a Ciência e Tecnologia (FCT) Ph.D. Scholarship PD/BD/113716/2015. This work is also financed by FCT within SusCity project (MITPTB/CS/0026/2013)

and GREsBAS project (SmartGP/0003/2015) under the framework of ERA-Net Smart Grids Plus.

References

[1] Oconnell N, Pinson P, Madsen H, Omalley M. Benefits and challenges of electrical demand response: A critical review. Renew Sustain Energy Rev 2014;39:686–99. http://dx.doi.org/10.1016/j.rser.2014.07.098.

[2] Torriti J, Hassan MG, Leach M. Demand response experience in Europe: Policies, programmes and implementation. Energy 2010;35:1575–83. http://dx.doi.org/10.1016/j.energy.2009.05.021.

[3] D'hulst R, Labeeuw W, Beusen B, Claessens S, Deconinck G, Vanthournout K. Demand response flexibility and flexibility potential of residential smart appliances: Experiences from large pilot test in Belgium. Appl Energy 2015;155:79–90. http://dx.doi.org/10.1016/j.apenergy.2015.05.101.

[4] Vanthournout K, Dupont B, Foubert W, Stuckens C, Claessens S. An automated residential demand response pilot experiment, based on day-ahead dynamic pricing. Appl Energy 2015;155:195–203. http://dx.doi.org/10.1016/j.apenergy.2015.05.100.

[5] Bessa RJ, Matos MA. Global against divided optimization for the participation of an EV aggregator in the day-ahead electricity market. Part II: Numerical analysis. Electr Power Syst Res 2013;95:309–18. http://dx.doi.org/10.1016/j.epsr.2012.08.013.

[6] Bessa RJ, Matos MA, Soares FJ, Lopes JAP. Optimized bidding of a EV aggregation agent in the electricity market. IEEE Trans Smart Grid 2012;3:443–52. http://dx.doi.org/10.1109/TSG.2011.2159632.

[7] Kristoffersen TK, Capion K, Meibom P. Optimal charging of electric drive vehicles in a market environment. Appl Energy 2011;88:1940–8. http://dx.doi.org/10.1016/j.apenergy.2010.12.015.

[8] Vagropoulos SI, Bakirtzis AG. Optimal bidding strategy for electric vehicle aggregators in electricity markets. IEEE Trans Power Syst 2013;28:4031–41. http://dx.doi.org/10.1109/TPWRS.2013.2274673.

[9] Mohsenian-Rad H. Optimal demand bidding for time-shiftable loads. IEEE Trans Power Syst 2015;30:939–51. http://dx.doi.org/10.1109/TPWRS.2014.2338735.

[10] Ayón X, Gruber JK, Hayes BP, Usaola J, Prodanović M. An optimal day-ahead load scheduling approach based on the flexibility of aggregate demands. Appl Energy 2017;198:1–11. http://dx.doi.org/10.1016/j.apenergy.2017.04.038.

[11] Chen S, Chen Q, Xu Y. Strategic bidding and compensation mechanism for a load aggregator with direct thermostat control capabilities. IEEE Trans Smart Grid 2016;3053:1–10. http://dx.doi.org/10.1109/TSG.2016.2611611.

[12] Babar M, Nguyen PH, Cuk V, Kamphuis IG, Bongaerts M, Hanzelka Z. The evaluation of agile demand response: an applied methodology. IEEE Trans Smart Grid 2017;3053. http://dx.doi.org/10.1109/TSG.2017.2703643. 1-1.

[13] Saez-Gallego J, Morales JM, Zugno M, Madsen H. A data-driven bidding model for a cluster of price-responsive consumers of electricity. IEEE Trans Power Syst 2016;31:5001–11. http://dx.doi.org/10.1109/TPWRS.2016.2530843.

[14] Perfumo C, Kofman E, Braslavsky JH, Ward JK. Load management: Model-based control of aggregate power for populations of thermostatically controlled loads. Energy Convers Manage 2012;55:36–48. http://dx.doi.org/10.1016/j.enconman.2011.10.019.

[15] Mathieu JL, Member S, Koch S, Member S, Callaway DS. State estimation and control of electric loads to manage real-time energy imbalance. 2013; 28: 430–40.

[16] Callaway DS. Tapping the energy storage potential in electric loads to deliver load following and regulation, with application to wind energy. Energy Convers Manage 2009;50:1389–400. http://dx.doi.org/10.1016/j.enconman.2008.12.012.

[17] Zhou Y, Wang C, Wu J, Wang J, Cheng M, Li G. Optimal scheduling of aggregated thermostatically controlled loads with renewable generation in the intraday electricity market. Appl Energy 2017;188:456–65. http://dx.doi.org/10.1016/j.apenergy.2016.12.008.

[18] Subramanian A, Garcia MJ, Callaway DS, Poolla K, Varaiya P. Real-time scheduling of distributed resources. IEEE Trans Smart Grid 2013;4:2122–30. http://dx.doi.org/10.1109/TSG.2013.2262508.

[19] Vasirani M, Kota R, Cavalcante RLG, Ossowski S, Jennings NR. An agent-based approach to virtual power plants of wind power generators and electric vehicles. IEEE Trans Smart Grid 2013;4:1314–22. http://dx.doi.org/10.1109/TSG.2013.2259270.

[20] Babar M, Nyugen PH, Cuk V, Kamphuis IGR, Bongaerts M, Hanzelka Z. The rise of AGILE demand response: Enabler and foundation for change. Renew Sustain Energy Rev 2016;56:686–93. http://dx.doi.org/10.1016/j.rser.2015.11.084.

[21] Daily and Intraday Electricity Market Operating Rules. http://www.omie.es/files/20151223_reglas_mercado_ingles.pdf; 2015 [accessed 05.07.17].

[22] EPEX, GME, N. Pool, OMIE, OPCOM, OTE, TGE, EUPHEMIA Public Description. https://www.nordpoolspot.com/globalassets/download-center/pcr/euphemia-public-documentation.pdf; 2015 [accessed 05.07.17].

[23] Barquín J, Rouco L, Rivero E. Current designs and expected evolutions of Day-ahead, Intra-day and balancing market/ mechanisms in Europe. OPTIMATE: Eur. Proj; 2011.

[24] Redes Energéticas Nacionais (REN), Manual de Procedimentos do Acerto de Contas, [In Port. (2008). http://www.mercado.ren.pt/EN/Electr/MarketInfo/Document/BibSubregula/MPACDezembro2008.pdf.

[25] Soares T, Pinson P, Jensen TV, Morais H. Optimal offering strategies for wind power in energy and primary reserve markets. IEEE Trans Sustain Energy 2016;7:1036–45. http://dx.doi.org/10.1109/TSTE.2016.2516767.

[26] Wang Q, Zhang C, Ding Y, Xydis G, Wang J, Østergaard J. Review of real-time electricity markets for integrating Distributed Energy Resources and Demand Response. Appl Energy 2015;138:695–706. http://dx.doi.org/10.1016/j.apenergy.2014.10.048.

[27] Sauba G, Van Der Burgt J, Varvarigos E, Makris P, Schoofs A. VIMSEN - Smart tool for energy aggregators. In: INTELEC, Int. Telecommun. Energy Conf. 2016; 2016. http://dx.doi.org/10.1109/INTLEC.2015.7572272.

[28] Jacobsen RH, Gabioud D, Basso G, Alet PJ, Azar AG, Ebeid ESM. SEMIAH: An aggregator framework for european demand response programs. In: Proc. - 18th Euromicro Conf. Digit. Syst. Des. DSD 2015; 2015. p. 470–7. http://dx.doi.org/10.1109/DSD.2015.96.

[29] Radecki P, Hencey B. Online building thermal parameter estimation via unscented kalman filtering, 2012 Am. In: Control Conf. (2012) p. 3056–62. doi: 10.1109/acc.2012.6315699.

[30] Bianchini G, Casini M, Vicino A, Zarrilli D. Demand-response in building heating systems: A Model Predictive Control approach. Appl Energy 2016;168:159–70. http://dx.doi.org/10.1016/j.apenergy.2016.01.088.

[31] Ma Y, Kelman A, Daly A, Borelli F. Predictive control for energy efficient buildings with thermal storage. IEEE Control Syst 2012; 44–64. doi: 10.1109/MCS.2011.2172532.

[32] Fujitsu, Split type air conditioners, (n.d.). http://www.fujitsuklime.com/wf-proizvodi/3/fujitsu-klima-uredjaj-zidni-inverter-asyg12luca-aoyg12luca-katalog.pdf [accessed 27.10.16].

[33] Iria JP, Soares FJ, Bessa RJ. Optimized demand response bidding in the wholesale market under scenarios of prices and temperatures. 2015 IEEE Eindhoven PowerTech. PowerTech 2015; 2015. doi:10.1109/PTC.2015.7232428.

[34] Pinson P, Madsen H, Nielsen HA, Papaefthymiou G, Klockl B. From probabilistic forecasts to statistical scenarios of short-term wind power production. Wind Energy 2009;12:51–62. http://dx.doi.org/10.1002/we.284.

[35] meteogalicia. http://www.meteogalicia.gal/web/index.action; n.d. [accessed 26.07.17].

[36] Soares FJ, Lopes JAP, Almeida PMR. A stochastic model to simulate electric vehicles motion and quantify the energy required from the grid. In: 2011 17th Power Syst. Comput. Conf.; 2011. p. 22–26. http://www.pscc-central.org/uploads/tx_ethpublications/fp359.pdf.

[37] Filipe Soares. Impact of the deployment of electric vehicles in the grid operation and expansion. Faculty of Engineering of University of Porto; 2011.

[38] Redes Energéticas Nacionais (REN), Load Profiles. http://www.mercado.ren.pt/EN/Electr/MarketInfo/Load/Pages/LoadProfiles.aspx; n.d. [accessed 28.10.16].

[39] ERSE (Portuguese energy Regulator), Profiles of losses, load, selfconsumption and generation (in Portuguese). http://www.erse.pt/pt/electricidade/regulamentos/acessoasredesaasinterligacoes/Paginas/PerfishorariosdeperdasedeconsumoemBTEBTNeIP.aspx?master=ErsePrint.master; n.d. [accessed 27.07.17].

[40] U.S. Department of Energy (DOE), Building America Analysis Spreadsheets, n.d.

[41] Agnetis A, Dellino G, Detti P, Innocenti G, De Pascale G, Vicino A. Appliance operation scheduling for electricity consumption optimization. In: Proc. IEEE Conf. Decis. Control; 2011. p. 5899–5904. doi: 10.1109/CDC.2011.6160450.

[42] Hastie T, Tibshirani R, Friedman J. The elements of statistical learning, 2nd ed. Springer; 2009. doi: 10.1198/jasa.2004.s339.

[43] Pedregosa F, Varoquaux G, Gramfort A, Michel V, Thirion B, Grisel O, et al. Scikit-learn: Machine Learning in Python. J. Mach. Learn. Res. 2012;12:2825–30. http://dx.doi.org/10.1007/s13398-014-0173-7.2.

[44] European Network of Transmission System Operators for Electricity (ENTSO-E), ENTSO-E Transparency Platform. https://transparency.entsoe.eu/; n.d. [accessed 28.10.16].

[45] Cui C, Wu T, Hu M, Weir JD, Li X. Short-term building energy model recommendation system: A meta-learning approach. Appl Energy 2016;172:251–63. http://dx.doi.org/10.1016/j.apenergy.2016.03.112.

[46] Niknam T, Azizipanah-Abarghooee R, Narimani MR. An efficient scenario-based stochastic programming framework for multi-objective optimal micro-grid operation. Appl Energy 2012;99:455–70. http://dx.doi.org/10.1016/j.apenergy.2012.04.017.